Sputtered SiO_2 as low acoustic impedance material for Bragg mirror fabrication in BAW resonators

J. Olivares, E. Wegmann, J. Capilla, E. Iborra, M. Clement
GMME. Universidad Politécnica de Madrid
Madrid, Spain

L. Vergara
ICMM-CSIC
Madrid, Spain

R. Aigner
TriQuint Semiconductor.
Apopka, Florida, USA

Abstract— **In this paper we describe the procedure to sputter low acoustic impedance SiO_2 films to be used as low acoustic impedance layer in Bragg mirrors for BAW resonators. The composition and structure of the material are assessed through infrared absorption spectroscopy. The acoustic properties of the films (mass density and sound velocity) are assessed through X-ray reflectometry and picosecond acoustic spectroscopy. A second measurement of the sound velocity is achieved through the analysis of the longitudinal λ/2 resonance that appears in these silicon oxide films when used as uppermost layer of an acoustic reflector placed under an AlN-based resonator.**

I. INTRODUCTION

Bulk acoustic wave resonator technology is a recent solution for low cost, high performance bandpass filters for digital wireless communications, such as wireless networking, cellular phones, or global positioning systems. These filters are composed of several resonators electrically connected to obtain the desired filter characteristics. To obtain well-performing devices, a good acoustic isolation of the resonators must be achieved to avoid energy losses that reduce their quality factor. There are two typical methods to achieve a good acoustic isolation. The first one consists in creating an air gap between the resonator and the substrate; as the acoustic radiation to the air is minimal, energy losses can only take place through the supports. These structures, called film bulk acoustic resonators (FBAR), have serious drawbacks, as a complex fabrication technology or a too high thermal isolation that limits the power handling. The alternative method is the use of acoustic reflectors between the resonators and the substrate; the resulting structures are called solidly mounted resonators (SMR). Bragg mirrors are typical acoustic reflectors, formed by piling films with a thickness of a quarter of the wavelength (λ/4) of the resonant wave, alternating low and high acoustic impedance materials. The acoustic impedance of a material is defined as the product of its mass density and the sound velocity of the wave in the solid. Typical materials with high acoustic impedance are, thus, dense and stiff, as is the case with some metals like platinum (Pt) [1], molybdenum (Mo) [2], or tungsten (W) [3]. To build insulating Bragg mirrors tantalum pentoxide (Ta_2O_5) [1], aluminum nitride (AlN) [4], or silicon nitride (Si_3N_4) [5] can be used, as long as they are combined with very-low acoustic impedance layers. The most commonly used low acoustic impedance material is silicon dioxide (SiO_2), because of its easy processing and full compatibility with standard silicon technologies. Other low impedance materials like aluminum (Al) [6] and silicon oxicarbide (SiOC) [5] have also been used, although to a lesser extent, owing to the high acoustic losses of SiOC and the metallic character of Al.

Some investigations on the deposition of porous silicon dioxide as a low-*k* dielectric were undertaken in the nineties [7]. Owing to their porous structure, these oxides exhibit mass densities lower than that of conventional thermally-grown silicon oxides (2.2 g/cm^3). Besides, a reduction in the elastic coefficients of the material is also reported [8], which suggests that longitudinal sound waves in porous oxides travel very likely at velocities lower than 6100 m/s, which is the longitudinal velocity in standard SiO_2. For these two reasons, the acoustic impedance of porous SiO_2 is expected to be significantly lower than that of conventional SiO_2.

In this work we describe the procedure to deposit silicon oxide layers with low acoustic impedance by reactive sputtering. The structure, density and sound velocity of this material have been assessed by different techniques, which include the fabrication and characterization of specific devices, in order to check whether these layers can improve the performance of SiO_2-based Bragg mirrors by providing higher acoustic impedance mismatch.

II. EXPERIMENTAL

Silicon oxide films were deposited in a Leybold Z-550 system by pulsed-DC magnetron sputtering of a Si target with a diameter of 150 mm in Ar/O_2 admixtures. Bare (100)-Si wafers and Si wafers covered with Mo thin films were used as substrates. The pulsed-DC power applied to the target was set to 1200 W and its frequency to 50 kHz with a duty cycle of 75%. The films were optimized by varying the total pressure in the chamber (between 1.5 mTorr and 9 mTorr) and the percentage of O_2 in the gas (between 10% and 80%). The combination of a mechanical shield for the target and an oscillating substrate-holder allowed to deposit films with a thickness uniformity better than 5% within a 100 mm Si wafer.

*contact author J.O.: olivares@etsit.upm.es

The thickness of the films was measured with a Veeco Dektak 150 profilometer. Infrared transmission spectra were measured at room temperature with a Fourier transform infrared (FTIR) Nicolet 5-PC spectrophotometer in the transmission mode. We used non-polarized light at normal incidence over the 400 cm^{-1} to 4000 cm^{-1} range with a spectral resolution of 4 cm^{-1}. The Si absorption bands corresponding to the substrate were eliminated from the FTIR spectrum by subtracting the spectrum measured in a bare Si wafer.

The density of the SiO_2 layers was assessed by X-ray reflectometry (XRR) measurements using a Supratech XPERT-PRO diffractometer operated at grazing incidence between 0.05º and 2.5º. The experimental data were fitted using the commercial software RCREFSimW from IHP [9], which provides the density of the layers as well as their thickness.

The sound velocity was assessed in different test structures by the picosecond ultrasonic technique, in a Metapulse system from Rudolf Technologies. The acoustic velocity of the films was also determined by measuring specific SMR structures containing the films SiO_2 under study. These films were sputtered as the uppermost layer of high quality Bragg mirrors made of tungsten and conventional SiO_2 deposited by CVD. The sound velocity was derived from the thickness of the layer and the resonant frequency of the λ/2 resonance induced in it. These SMR test devices were measured with an Agilent network analyzer PNA N5230A between 300 MHz and 4 GHz using a probe station with Picoprobe test probes.

III. CHARACTERIZATION OF SPUTTERED SILICON OXIDE

A. *Sputtering process*

We have investigated the reactive sputtering process of a Si target in different Ar/O_2 mixtures. Fig. 1 shows the variation of the deposition rate and of the target voltage as a function of the oxygen content in the gas discharge for a pressure of 9 mTorr and a power of 1200 W. Two regimes of extraction of the material, defined by the oxidation of the target surface [10], can be clearly distinguished. At low oxygen contents, the sputter rate of the target is larger than the oxidation rate of its surface. This prevents the formation of a silicon oxide layer on the surface of the target, leading to the *metal regime*, characterized by a high deposition rate and a high target voltage. As the partial pressure of oxygen is increased, a threshold is reached at which the rate of oxidation of the surface of the target exceeds the rate of removal, and a silicon oxide layer, characteristic of the *poisoned regime*, covers the surface of the target. As can be observed in Fig. 1, this threshold is marked by a sharp decrease in the deposition rate. This decrease can be accounted for by three different phenomena. Firstly, it is due in part to the fact that silicon oxide has a lower sputtering yield than silicon. Additionally, silicon oxide has higher secondary-electron emission yield than silicon. At a constant power supply, the increased secondary electron current automatically decreases the target voltage as shown in the Fig. 1. Finally, a third cause of the drop in the sputtering rate is the less efficient sputtering by oxygen ions than by Ar ions.

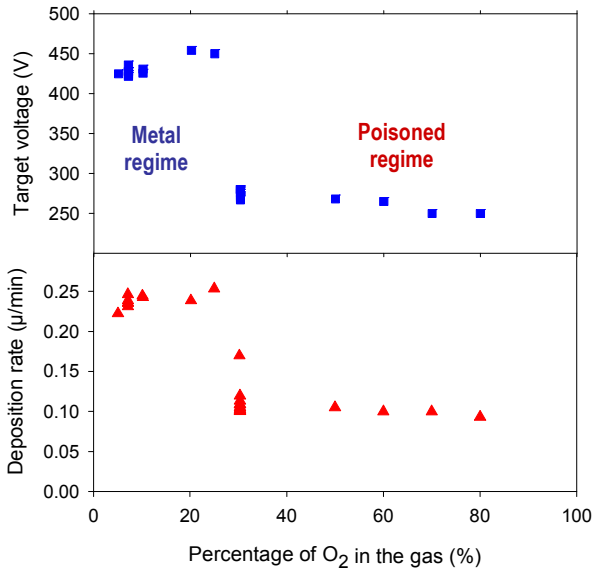

Figure 1. Deposition rate and target voltage as a funtion of the O_2 content in the discharge for different sputter processes carried out at at a pressure of 9 mTorr and a power of 1200 W

B. *Structure and composition of sputtered oxides*

The composition of the sputtered films has been assessed by infrared absorption spectroscopy. The typical spectra of some representative films (all of them with identical thicknesses) obtained in the *metal* and *poisoned regimes* are shown in Fig. 2, together with a spectrum of a thermal oxide film, for comparison.

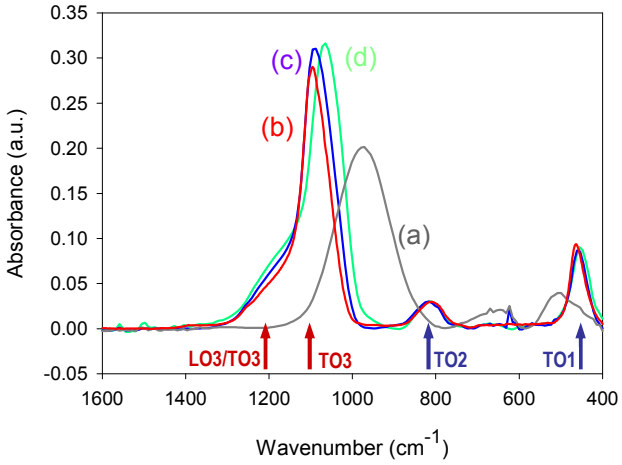

Figure 2. Infrared absorbance spectra of films deposited in the *metal regime* (a) and in the poisoned regime (c) and (d). Spectrum (b) corresponds to silicon dioxide film grown by thermal oxidation.

It can be observed that the spectra of the films deposited in each of the two extraction regimes are significantly different. Spectrum (a), corresponding to a film deposited in the *metal regime*, exhibits a wide absorption band centred at around 980 cm^{-1}, which is characteristic of SiO films [11]. This result demonstrates that silicon oxide films deposited under the *metal regime* tend to be silicon-rich. On the contrary, spectra (c) and (d), corresponding to films deposited in the *poisoned regime*, and (b) corresponding to a thermal SiO_2 film, present

features characteristic of SiO_2 films: the TO1 rocking mode at 460 cm^{-1}, the TO2 bending mode at 800 cm^{-1}, and the TO3 antisymmetric stretching mode between 1060 cm^{-1} and 1080 cm^{-1} [12,13]. Additionally, this last mode exhibits a shoulder at around 1200 cm^{-1}, which has been attributed to a coupling of LO-TO modes with a dominant LO character [14] (although a contribution of the transversal optical TO4 mode, related to a disordered structure, has also been reported [15,16]).

A closer inspection of the absorption spectra (c) and (d) reveals some slight differences between the films deposited in the *poisoned regime*, regarding especially the position of the TO3 mode and the intensity of its shoulder. The TO3 mode of film (d) appears at a lower wavenumber and its shoulder shows a higher intensity, as compared to the TO3 mode of film (c). Several factors have been reported to influence the position of the TO3 mode. First, a shift of the TO3 band from 1072 cm^{-1} to 1095 cm^{-1} has been found in thermal SiO_2 films of high quality (compact, stoichiometric and defect-free) as their thickness is increased from 10 nm to 800 nm. Besides, the shift of the TO3 mode is accompanied by an increase in its intensity, which is more significant than that in the intensity of its shoulder [17]. Secondly, a linear shift of the TO3 mode towards higher energies has also been observed in nearly stoichiometric SiO_x films (with x~2) as the oxygen content is increased [18]. Finally, a shift of the TO3 mode towards lower wavenumbers and the increase of the intensity of its shoulder have also been related to an increase of the porosity of the film [14, 19].

To determine which of these three factors is responsible for the shifts observed in the TO3 mode, we have inspected the TO1 and TO2 modes, whose position depends on the composition of the film, but not on its disorder or its porosity. We observe that the position of these modes is the same for the sputtered SiO_2 films and for the thermal oxide film, which indicates that all the films analyzed here have a composition very close to stoichiometric SiO_2 [17]. Additionally, the intensity of all the TO modes is roughly the same, as was to be expected (since we chose for this analysis samples with the same thickness). On the other hand, we observe that the shift of the TO3 mode is accompanied by a significant increase in the shoulder intensity. All these results indicate that the shift of the TO3 mode to lower wavenumbers is very likely due to an increase in the porosity.

The structural variations of the SiO_2 films deposited in the two sputter regimes were also evidenced by their different behavior in BHF etching solutions. Fig. 3 shows the deposition rate and the etch rate of a large variety of SiO_x films depicted as a function of the wavenumber of the TO3 mode. Films deposited at high rates under the *metal regime*, with compositions close to SiO and the main IR absorption band always below 1000 cm^{-1}, are insoluble in BHF. Among the films deposited at low rates in the *poisoned regime*, two distinct behaviors are observed. The first family of films, with TO3 bands at around 1072 cm^{-1} and significantly intense shoulders, have very high etch rates (5.5 µm/min), which confirms the porous structure pointed out by their IR absorption spectra. A second family of films, whose LO3 band is shifted to around 1080 cm^{-1} (closer to that of thermal oxide) and that present a smaller shoulder, exhibits notably lower etch rates (0.25 µm/min), which is in agreement with a less porous structure.

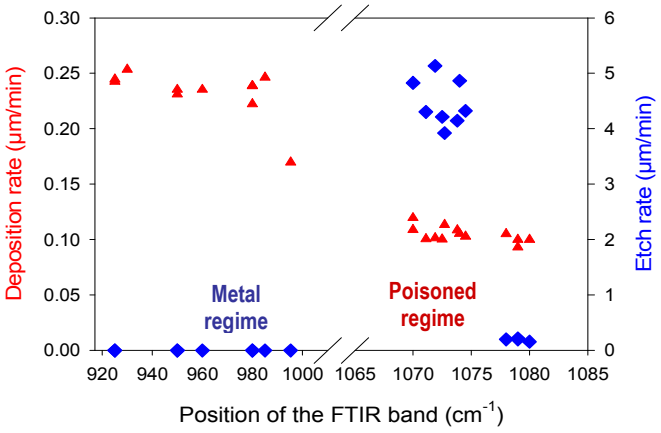

Figure 3. Deposition rates versus the position of the main absorption band of the IR spectra of films deposited at 1200 W. The total pressure and the gas composition were not the same for all the films.

C. *Density assessment*

We have focused on films grown in the *poisoned regime*, as their structural changes very likely cause variations in their acoustic properties. We have first determined the density of these SiO_2 films by XRR measurements, whose main advantage is that they provide a direct assessment of the density of a thin film independently of its thickness. When the X-ray beam impinges from the air onto a flat surface with an incident angle below a critical angle θ_c, the beam is totally reflected. When the incident angle exceeds θ_c, the X-rays penetrate into the film and the intensity of the reflected beam drops sharply. If θ_c and the wavelength λ of the X-rays are known, the mass density ρ can be obtained through the equation

$$\rho = \frac{\pi \cdot \theta_c^2}{r_e \cdot \lambda^2} \qquad (1)$$

where r_e is the radius of the electron.

These measurements, shown in Fig. 4, were carried out for three different samples, a thermal SiO_2 layer (used as reference) and two silicon oxides of different porosity. The fitting of the experimental data using the commercial software RCREFSimW from IHP allowed to determine accurately the critical angle θ_c and, hence, the mass density ρ. It can be observed that the critical angle for the porous sputtered film (a) is significantly lower than for the thermal oxide film, whereas that of film (b) has an intermediate value. The density derived from the fitting of the experimental curves is 1.8 g/cm^3 for the porous film (a), 2.1 g/cm^3 for film (b), and 2.2 g/cm^3 for the thermal oxide film; the latter agrees perfectly with the density of conventional thermal oxide films. These results confirm the porous structure of some films sputtered in the *poisoned regime*, exhibiting significant shifts of the TO3 mode to lower wavelengths. Under these conditions, we were

able to achieve films with densities 18% lower than that of conventional silicon oxides.

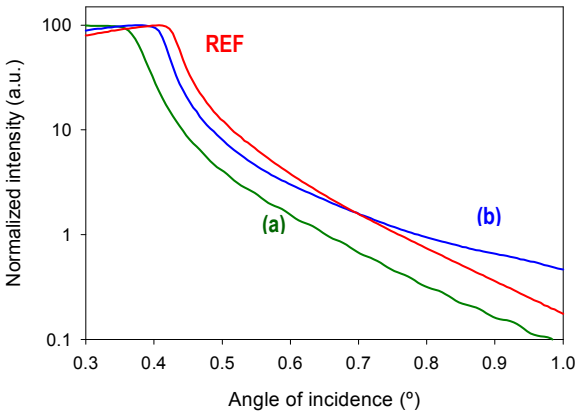

Figure 4. X-ray reflection curves of a reference thermal oxide (REF, in red), a high-etch rate SiO_2 films (a, in blue), and. a low-etch rate SiO_2 film (b, in green).

D. Sound velocity assessment

The sound velocity of the porous SiO_2 films was assessed using two different techniques.

1) BAW resonators assessment

To assess the longitudinal sound velocity in our SiO_2 films, we have investigated the λ/2 mode that appears in these layers when they are used as the uppermost reflector layer in a conventional SMR structure. This λ/2 mode is a stationary wave stimulated by the piezoelectric resonator inside the SiO_2 layer. Taking into account that the wavelength of the stationary is twice the thickness of the layer, the sound velocity v_s of the SiO_2 porous films can be directly derived from the resonant frequency of the λ/2 mode using the equation

$$v_S = f \times 2t \qquad (2)$$

where f is the resonant frequency and t the thickness of the films.

In order to carry out this kind of experiments, we have fabricated AlN-based BAW resonators on top of Bragg mirrors supplied by TriQuint Semiconductor, which alternate five reflector layers formed by low acoustic impedance films of conventional SiO_2 deposited by CVD, and high acoustic impedance tungsten films deposited by sputtering. To evaluate the longitudinal sound velocity of sputtered porous SiO_2, we replaced the uppermost CVD SiO_2 layer of the Bragg mirror by layers of porous SiO_2 of different thicknesses. The BAW resonators consisted of an iridium bottom electrode evaporated on top of a Ti seed layer to improve the adhesion of the Ir layers to the silicon oxide, an AlN piezoelectric film whose thickness was tuned to the central frequency of the Bragg mirror, and a Mo top electrode. The top electrode was patterned, whereas the bottom electrode was kept continuous. To access the iridium bottom electrode, vias were opened in the AlN by wet etching in KOH solutions. Fig. 5 shows a sketch of the test structures fabricated to assess the longitudinal sound velocity in the sputtered SiO_2 layer.

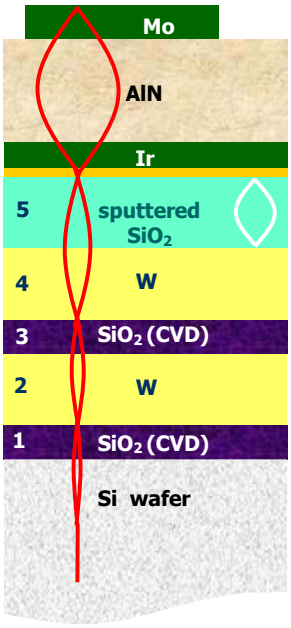

Figure 5. Sketch of the test devices used for assessing the sound velocity in sputtered SiO_2 films. The main resonant mode in the piezoelectric is shown in red, and the λ/2 mode in the SiO_2 film in white.

The modulus of the impedance of the different BAW resonators containing SiO_2 porous layers of different thicknesses is shown in Fig. 6. The main resonance frequency is around 1.5 GHz, whereas the frequency of the λ/2 mode of the upper SiO_2 layer varies between 2 GHz and 3 GHz, depending on the thickness of the SiO_2 layer. The frequency of the λ/2 modes was determined experimentally and the sound velocity calculated through equation (2). The values obtained for a large set of resonators are shown in Fig. 7.

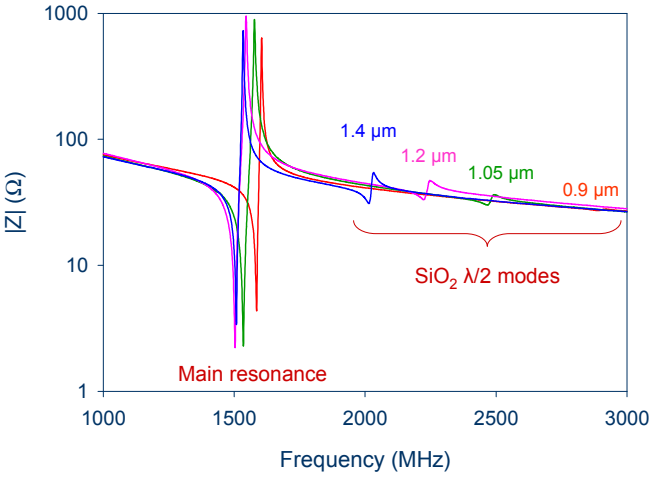

Figure 6. Modulus of the impedance versus frequency for several resonators with sputtered SiO_2 of different thicknesses.

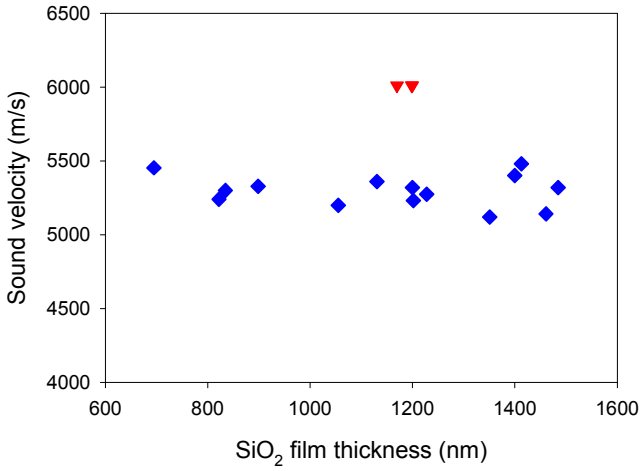

Figure 7. Sound velocity for sputtered SiO_2 films as a function of their thickness. Triangles represent the sound velocity obtained for CVD-SiO_2 reference films.

The data in Fig. 7 confirm that the decrease of ρ in porous films is accompanied by a reduction in their sound velocity, whose mean value is around 5350 m/s, 11% lower than that of the CVD SiO_2 reference films (6010 m/s).

The overall response of the resonator was fitted to the Mason's one-dimensional model. The material constants used for the fittings were previously tested in other devices, except for the sputtered SiO_2 film, whose mass density was taken from XRR measurements. The fitting of the data confirmed in all the cases the presence of the $\lambda/2$ mode in the SiO_2 layer at the detected frequency.

The values of the mass density and sound velocity yield an acoustic impedance of the sputtered SiO_2 films of 9.5×10^6 $N \cdot s/m^3$, which is around a 30% lower than that of conventional SiO_2 films used in Bragg mirrors.

2) Picosecond ultrasonic measurements

An alternative way of assessing the sound velocity is by the picosecond ultrasonic technique [20], whose experimental set-up is shown in Fig. 8.

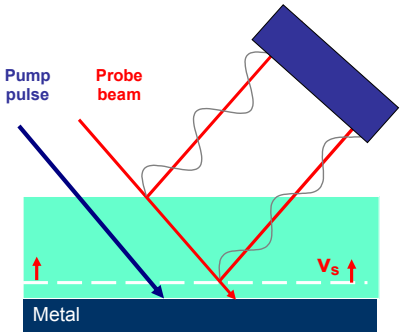

Figure 8. Experimental set-up for picosecond ultrasonic measurements

In this method, an optical pulse, called pump pulse, heats the surface of the sample producing a local dilatation. This generates a longitudinal strain wave, which propagates through the film at the longitudinal sound velocity. In the case of an optically transparent film, such as SiO_2 films deposited on opaque substrates, the sound wave is generated at the opaque interface. As the strain wave travels up trough the transparent film, it causes local variations of the refractive index. These changes can be detected by a second beam, called the beam probe. The beam probe reflected at the surface of the films interferes with the beam reflected at the front of the traveling strain wave, causing the intensity of the signal in the detector to oscillate with time. The period T of the so-called Brillouin oscillations is directly related to the longitudinal sound velocity through the equation,

$$v_s = \frac{\lambda}{2nT\cos\theta} \qquad (3)$$

where λ is the wavelength of the probe beam, n the refractive index of the dielectric layer at λ and θ the incident angle.

These measurements were carried out on test structures composed of SiO_2 porous layers of different thicknesses deposited on top of molybdenum substrates. The Brillouin oscillations in one of these samples is shown in Fig. 9.

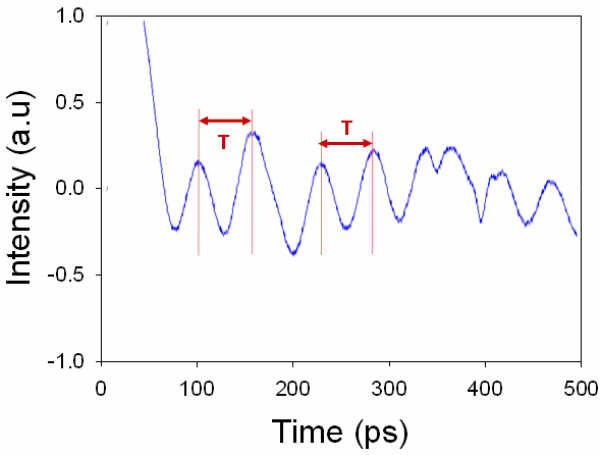

Figure 9. Brillouin oscillations of the detected signal from a SiO_2/Mo structure using picosecond ultrasonics

The sound velocity measured in several SiO_2 films deposited on Mo substrates has a mean value of 5450 m/s. The slight difference in the values of the sound velocities obtained by the two techniques could be attributed to the use of different substrates for the growth of the SiO_2 films, although it is within the experimental uncertainty.

IV. Conclusions

In this paper we analyze porous SiO_2 films deposited by pulsed-DC sputtering in Ar/O_2 atmospheres. Their porosity leads to a reduction in the mass density and the longitudinal

sound velocity, which leads to an acoustic impedance lower than that of conventional SiO_2. Their sound velocity has been derived from the $\lambda/2$ overmode that appears when they are used as the uppermost layer of the Bragg mirror in a BAW resonator. Values of the density up to 18% lower than that of thermal oxide, and values of the sound velocity 12% lower than for conventional CVD SiO_2. This represents a reduction of the acoustic impedance of 30%.

This material allows the fabrication of Bragg mirrors for BAW resonators with better performance than in the case of the compact SiO_2 commonly used as low impedance material for this application.

ACKNOWLEDGMENT

This work has been supported by the Ministerio de Educación y Ciencia of Spain through project MAT2007-62162, and by the Comunidad de Madrid and the UPM through the IV PRICIT programme and by the European Union through the European Regional Development Fund (FEDER).

REFERENCES

[1] R.Strijbos, A.Jansman, J.-W. Lobeek, N. Xin Li, and N. Pulsford, "Design and Characterisation of High-Q Solidly-Mounted Bulk Acoustic Wave Filters", Proc. 2007 Electronic Components and Technology Conference pp.169-174.

[2] C.-J. Chung, Y.-C. Chen, C.-C. Cheng, K.-S. Kao, "Fabrication and frequency response of solidly mounted resonators with 1/4λ mode configuration", Thin Solid Films 516 (2008) pp. 5277–5281

[3] R. Aigner, J. Kaitil, J. Ella, L. Elbrecht, W. Nessler, M. Handtmann, T.-R. Herzog, and S. Marksteiner, "Bulk-Acoustic-Wave Filters: Performance Optimization and Volume Manufacturing", Proc. 2003 IEEE MIT-S Digest, pp. 2001-2004.

[4] S.H. Kim, J.H. Kim, J.K. Lee, S.H. Lee, K. H. Yoon, "Bragg reflector thin film resonator using aluminium nitride deposited by rf sputtering", Proc. 2000 IEEE Microwave Conference Asia-Pacific, pp. 1535–1538.

[5] A. Reinhardt, N. Buffet, A.Shirakawa, J. B. David, G. Parat, M. Aid, S. Joblot, P. Ancey, "Simulation of BAW resonators frequency adjustment", Proc. 2007 IEEE Ultrasonics Symposium, pp. 1444-1447.

[6] J. Enlund, D. Martin, V. Yantchev and I. Katardjiev, "Solidly mounted thin film electro-acoustic resonator utilizing a conductive Bragg reflector", Sensors and Actuators A 141 (2008) pp. 598–602.

[7] C. Murraya, C. Flannery, I. Streiter, S.E. Schulz , M.R. Baklanov, K.P. Mogilnikov , C. Himcinschi , M. Friedrich , D.R.T. Zahn , T. Gessner, "Comparison of techniques to characterise the density, porosity and elastic modulus of porous low-k SiO xerogel films", Microelectronic Engineering 60 (2002) pp. 133–141.

[8] C. Murray, C. Flannery, I. Streiter, S.E. Schulz , M.R. Baklanov, K.P. Mogilnikov , C. Himcinschi , M. Friedrich , D.R.T. Zahn , T. Gessner, "Comparison of techniques to characterise the density, porosity and elastic modulus of porous low-k SiO xerogel films", Microelectronic Engineering 60 (2002) pp. 133-141

[9] P. Zaumseil, Reflectivity software RCRefSimW, Version 1.09 Innovations for high performance Microelectronics. Frankfurt Germany. (http://www.ihp-microelectronics.com)

[10] T. Kubart, O. Kappertz, T. Nyberg, S. Berg, "Dynamic behaviour of the reactive sputtering process", Thin Solid Films 515 (2006) pp. 421-424.

[11] G. Pérez, J.M. Sanz. « Infrared characterization of evaporated SiO thin films", Thin Solid Films 416 (2002) pp. 24-30.

[12] M. K. Gunde, "Vibrational modes in amorphous silicon dioxide", Physica B 292 (2000) pp. 286-295.

[13] P. Innocenzi, "Infrared spectroscopy of sol–gel derived silica-based films: a spectra-microstructure overview", Journal of Non-Crystalline Solids 316 (2003) pp. 309-319.

[14] R.M. Almeida and C.G. Pantano, "Structural investigation of silica gel films by infrared spectroscopy", J. Appl. Phys. 68(8) (1990) pp. 4225-4232.

[15] C. T. Kirk, "Quantitative analysis of the effect of disorder-induced mode coupling on infrared absorption in silica", Physical Review B 38(2) (1988) pp. 1255-1273.

[16] P. Lange, "Evidence for disorder-induced vibrational mode coupling in thin amorphous SiO2 films", J. Appl. Phys. 66 (1989) pp. 201-204.

[17] J. A. Moreno, B. Garrido, J. Samitier, J. R. Morante, "Analysis of geometrical effects on the behavior and longitudinal modes of amorphous silicon", J. Appl. Phys. 81(4) (1997) pp. 1933-1942.

[18] A. Barranco, F. Yubero, J. Cotrino, J.P. Espinós, J. Benítez, T.C. Rojas, J. Allain, T. Girardeau. J.P. Rivière, A.R. González-Elipe, "Low temperature synthesis of dense SiO2 thin films by ion beam induced chemical vapor deposition", Thin Solid Films 396 (2001) pp. 9-15 (2001).

[19] J.S. Chou, "Effect of porosity on infrared-absorption spectra of silicon dioxide", J. Appl. Phys. 77 (1994) pp. 1805-1807

[20] A. Devos and R. Côte, "Strong oscillations detected by picosecond ultrasonics in silicon:Evidence for an electronic-structure effect", Phys. Rev. B 70, 125208 (2004).